Calculation of Rock Pressure in Loess Tunnels Based on Limit Equilibrium Theory and Analysis of Influencing Factors

Cheng Danjiang[1,2], Hua Junfeng[1,2], Zhu Jianguo[1,2], Ji Yang[3] and Hu Zhaoguang[4,*]

[1]*Road & Bridge International Co., LTD., Beijing, 100027, China*
[2]*China Communication North Road & Bridge Co., LTD., Beijing, 100027, China*
[3]*The Second Construction Co., LTD. of China Construction First Group, Beijing, 100068, China*
[4]*Zhengzhou University of Aeronautics, Zhengzhou 450046, China*
E-mail: Huzhaoguang008@163.com
[*]*Corresponding Author*

Received 21 March 2023; Accepted 14 April 2023;
Publication 22 June 2023

Abstract

The research on the calculation method of tunnel envelope pressure is a key issue in the design of tunnel engineering support structure. Based on the limit equilibrium theory, this paper proposes a method to calculate the surrounding rock pressure in shallow buried loess tunnels. Firstly, based on the investigation of the damage mode of the loess tunnel surrounding rock and the field measurement results of the surrounding rock pressure, the damage mode of the loess tunnel is proposed, and then a method of calculating the surrounding rock pressure applicable to the shallow buried loess tunnel is derived according to the limit equilibrium condition of the tunnel square soil body and the side wedge; the basic mechanical parameters are known in this method, so only the rupture angle β needs to be determined, and the rupture angle calculation model in the shallow buried loess tunnel is proposed

European Journal of Computational Mechanics, Vol. 32_1, 1–30.
doi: 10.13052/ejcm2642-2085.3211

Three assumptions are made in the rupture angle calculation model, and the rupture angle calculation formula is derived according to the stress state on the slip surface of the surrounding rock; the pressure of the surrounding rock in the loess tunnel obtained by this method is compared with four methods, namely, the pressure theory of the surrounding rock in the existing loose body of Taishaki, the pressure formula of the deeply buried surrounding rock in the railroad tunnel design code, the Beer Baumann method, and the Xie Jiayi method, in order to verify the correctness and validity of the calculation method used, and to analyze the influence of different parameters on the surrounding rock pressure. The innovation of this paper lies in the derivation of a method for calculating the pressure in the surrounding rock of a shallow buried loess tunnel using the limit equilibrium theory, and also further proposes a formula for calculating the rupture angle. The pressure of surrounding rock decreases with the increase of static earth pressure coefficient, lateral pressure coefficient, friction angle and cohesion in soil, but the static earth pressure coefficient has a greater influence on the surrounding rock pressure. With the increase of sagittal span ratio, tunnel burial depth and soil weight, the surrounding rock pressure peaked with the increase of tunnel burial depth, and the surrounding rock pressure curve increased first and then decreased.

Keywords: Surrounding rock pressure, limiting equilibrium theory, shallow buried loess tunnel, rupture angle, damage mode.

1 Introduction

With the gradual promotion of the construction of a strong transportation country, the construction of highways and high-speed railroads in the central and western regions of China has ushered in a new boom, and the mileage of loess tunnel construction has increased rapidly [1]. Shallow buried tunnel is a tunnel project with shallow burial depth, where the bearing arch cannot be formed in the surrounding rock after excavation and the support structure bears all the earth pressure generated by the overlying soil. Loess will form visible surface cracks due to the development of vertical joints in the stratum, and the development pattern of the rupture surface of the stratum and the determination of the tunnel load after excavation of shallow buried loess tunnel has been a difficult problem for tunnel design calculation [2].

The study of the surrounding rock pressure has been a hot issue in the field of tunnel engineering. There have been many studies on rock pressure

in loess tunnels. Xiao X et al. established the boundary conditions of foundation bearing capacity and constructed the mathematical model of foundation bearing capacity by calculating the mechanical characteristic parameters of foundation, thus completing the mechanical characteristic analysis of foundation bearing capacity [3]; Kim Jong-bu et al. developed the failure mode of the loess tunnel in accordance to the technical traits of the shallow buried tunnel in the loess area, delivered the energy of the structural loess clearance, and improved the loose surrounding rock above the loess tunnel based on I have come up with a pressure formula. Moore-Coulomb Criterion and Analysis Method of Upper Bound We bound and obtained the optimal solution of the upper bound by Matlab algorithm [4]; Wang H et al. Numerical simulation studies on the tunneling process were performed using finite element software and the results were compared with field monitoring results. They suggested that the displacement of the tunnel's upper and lumbar arches increased over time, that the upper arch at the tunnel entrance was severely affected by excavation, and that the plastic zone of the surrounding rock upper and lower arches increased. concluded. On the other hand, the plastic hip arch zone was smaller [5]; According to the stress-strain variation law of undisturbed loess and the law of shear strength change with structural parameters, we show the internal relationship between structure and strength of loess and show that structure is the controlling factor of loess strength. shows that the structural parameter ratio and the loess intensity ratio correspond to a simple proportional relationship. That is, the stronger the structure, the stronger the soil [6]; Bagheri H et al. studied the buckling conduct of an isotropic and uniformly allotted rotating annular plate below uniform compression of the internal and outer edges and similarly assumed that the plate rotates with a steady angular velocity. Based on the theory of plates with first-order shear strain, this equation was applicable to thin and medium-thickness plates, yielding a complete equilibrium equation and associated plate boundary conditions [7].

The engineering aspects of a loess tunnel are it seems that exceptional from these of different rock tunnels, and the evaluation of the surrounding rock stress is usually the key to the diagram of the tunnel construction. This paper proposes the failure mode of a loess tunnel and then obtains a calculation technique of surrounding rock strain appropriate for a loess tunnel based totally on the restricted equilibrium circumstance of the tunnel quadrangle and facet wedge. It is primarily based on the investigation of surrounding rock failure mode and the discipline size outcomes of surrounding rock strain in Huangshi Tunnel. The technique calculates the surrounding rock strain and

stress in a loess tunnel through the usage of too-free too free sand theory, the railway tunnel sketch code, the platts theory, and the Xie Jiayi method. It then compares the effects of the 4 techniques to determine the accuracy and validity of the calculation approach and the outcomes of the range of parameters on the surrounding rock pressure. The static earth strain coefficient has a good sized influence on the surrounding rock pressure, however so do the lateral stress coefficient, adhesion, attitude of soil inside friction, and static soil stress coefficient. The surrounding rock stress progressively rises as the vector span ratio, tunnel depth, and soil weight increase. The surrounding rock pressure curve grows initially before decreasing as the tunnel depth deepens, reaching a maximum value.

2 Failure Mode and Monitoring Result Analysis of Loess Tunnel Surrounding Rock

2.1 Failure Mode

The failure mode of a shallow buried loess tunnel differs from that of different tunnels due to the loess' one-of-a-kind massive pore shape and vertical joint boom points [8]. In a shallow buried loess tunnel, the displacement of soil usually consists of two components. The trouble of the surrounding soil has an influence on the soil above the tunnel roof and under the floor in a unique range, and loess typically exhibits vertical joint features. so its displacement direction is usually vertically downward. However, the loose soil within a certain range of the tunnel side wall, due to the formation of a free surface caused by tunnel excavation, will have a convergent displacement toward the center direction of the tunnel face. Its failure displacement includes both horizontal and vertical directions [9]. On the other hand, Xiao et al. Based on the structural Microcoulomb model, studied the instability mechanism of loess tunneling, ad pointed out that the failure mode of loess tunneling can be determined comprehensively by combining the structural damage program and the plastic zone program [10]. The result is that at the relatively shallow depth of the loess tunnel, the slip surface of the surrounding rock first develops at a certain angle from the arch bottom to the tunnel apex and then toward the surface with a tendency of inward contraction is shown.

The failure modes of the surrounding rocks within the Loess Tunnel can be summarized as follows. The free floor shaped by using loess tunnel excavation redistributes the stresses of the surrounding rock in the tunnel and the soil reaches its energy restriction close to the biggest tunnel, width,

Figure 1 Typical tunnel surrounding rock cracking patterns.

Table 1 Tunnel fracture surface parameters

Tunnel	Depth of Burial	Horizontal Distance	Crack Depth	Inclination	$45^\circ + \phi/2$
Tongluochuan Tunnel	26	20	4.3	61	54
Gaoqiao Tunnel	33	33	4.2	63	56
Huanglong Village Tunnel	13	11	2.7	73	55

forming a crushing slip surface the slip surface gradually extends upward at a constant angle, and the ground above the tunnel slopes unevenly along the slip surface [11]. The fracture surface extends upward from the surface to a certain depth, and tensile stress is generated in the ground. When the tensile stress exceeds the tensile strength of the surface loess, tensile cracks are generated. Due to the existence of vertical joints of loess, tensile cracks are approximately vertical on the surface [12]. Typical site geophysical and pit exploration results are shown in Figure 1.

Analysis of Figure 1 and Table 1 shows that.

(a) The fracture surface of surrounding rock in the loess tunnel is composed of two parts, namely, the lower inclined closed shear fracture and the upper vertical tensile fracture, and the distribution of both of them in the soil is in the shape of "inverted eight".

(b) With the increase of tunnel depth, the location of surface cracks moves away from the tunnel axis and to both sides. The dip Angle of the shear slip plane under surface tension fractures is slightly greater than $45^\circ + \varphi/2$, which is because the vertical joint-induced fractures in loess preferentially develop in the vertical direction. In the absence of

geophysical data, the approximate fracture Angle of $45^\circ + \varphi/2$ can meet the safety reserve requirements [13].

2.2 Analysis of Surrounding Rock Pressure Monitoring Results

Steel-string type sensors have a very wide application in geotechnical engineering because of their good accuracy and sensitivity, high tolerance to external harsh environment, and high stability of measurement results. In view of the above reasons, the steel string type earth pressure box is selected for the monitoring of the surrounding rock pressure in this tunnel project. The principle is as follows: there is a taut steel string inside the steel string type earth pressure box, and there exists an initial frequency corresponding to it, under the action of external load, the vibration frequency of the steel string inside the pressure box will also change due to the action of tension. From the relevant mathematical physical knowledge, it is known that the following relationship exists between the vibration frequency of the steel string and the tension it is subjected to:

$$f = \frac{1}{2L}\sqrt{\frac{\sigma}{\rho}} \tag{1}$$

From Equation (1), it can be seen that for a given earth pressure box, the vibration frequency of the steel string is only related to the tensile stress to which it is subjected, and the tensile stress of the steel string comes directly from the action of external stress. Therefore, for practical engineering applications, it is usually necessary to calibrate the earth pressure box before formally starting the monitoring work, and the direct relationship between the vibration frequency of the steel chord and the pressure on the earth pressure box film can be obtained from the calibration results as follows:

$$f^2 - f_0^2 = KP \tag{2}$$

Where: P is the pressure on the pressure box film, f is the vibration frequency of the steel string under the action of load P, f_o is the initial frequency of the steel string, and K is the calibration factor.

Through the analysis of a massive quantity of subject-measured facts of the preliminary aiding surrounding rock stress of Zhengzhou-Xi 'a Passenger committed line, it is discovered that the surrounding rock strain is essentially manifested as pressure, that is, the style of surrounding rock extrusion in the tunnel after tunnel excavation. The genuine surrounding rock strain is no longer evenly disbursed alongside the perimeter of the cave, and its maximum value may appear in any part of the cave, which is caused by the uncertainty of

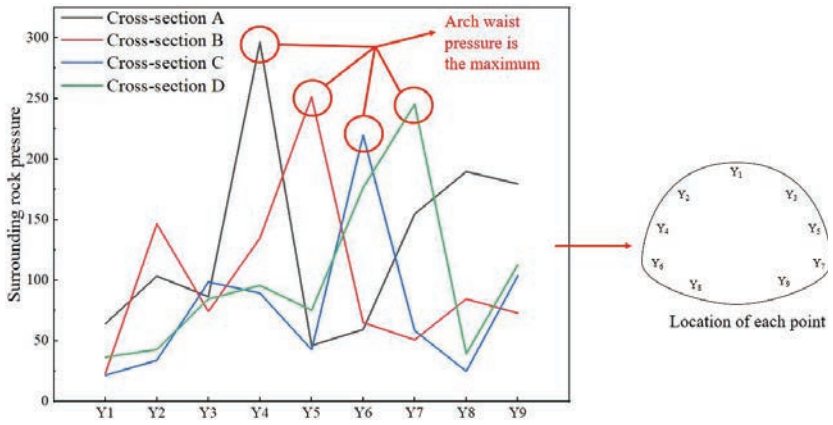

Figure 2 Distribution of pressure monitoring in different palm faces.

the formation conditions around the cave and the strength of the surrounding rock [14]. However, in general, the distribution personality of "cat ears" of surrounding rock stress in the loess tunnel is exceedingly obvious, and the most surrounding rock strain takes place in the waist as a substitute for the vault, as proven in Figure 2 (Y_i is the location of each monitoring point in different palm faces, and the corresponding contact pressure of the surrounding rock is in kPa.). This is regular with the authentic rupture Angle decided via subject investigation above, that is, from the floor to the most width of the tunnel facet wall (the soffit).

3 Calculation Method of Surrounding Rock Pressure in Loess Tunnel Based on Limit Equilibrium Theory

3.1 Basic Principle

The Mohr-Coulomb criterion itself is a strength criterion based on soil, which can reflect the different S-D effects of compressive strength and sensitivity to positive stresses of geotechnical materials more simply and clearly, and is more suitable for loose soils like loess. Moreover, compared with other strength codes with many empirical parameters, the Mohr-Coulomb criterion has only two material parameters, c and φ, which can be determined by various conventional experimental instruments and different methods. Therefore, the Mohr-Coulomb strength criterion is chosen as the theoretical basis for the derivation of the pressure calculation equation for the loess tunnel envelope in this paper.

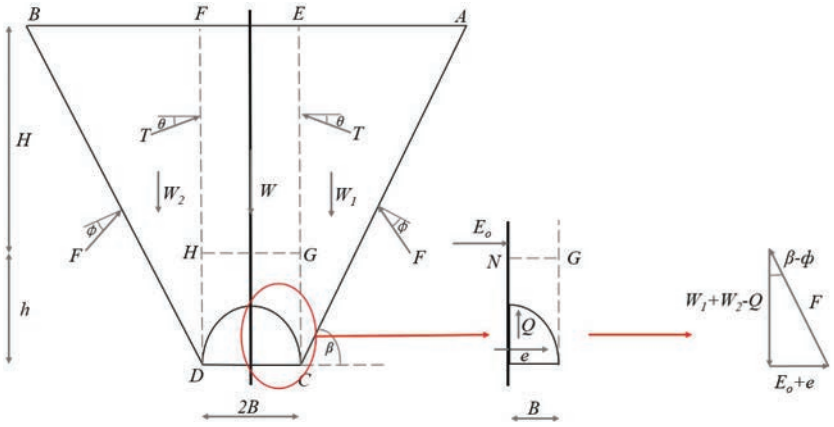

Figure 3 Failure mode of loess tunnel.

According to the existing conditions on the construction site, there are many micro-cracks around the guide tunnel, mainly distributed on both sides of the excavation face of the guide tunnel. The cracks extend diagonally upward along both sides of the tunnel to the top of the transverse passage, and the micro-crack propagation from the top of the transverse passage to the ground cannot be observed [15]. In order to prevent cracks from continuing to expand due to excessive settlement of the dome of the guide tunnel, temporary transverse and longitudinal steel supports are set in the guide tunnel, and micro-cracks are reinforced by grouting [16]. The failure mode of the loess tunnel is shown in Figure 3.

It is assumed that AC and BD are the fracture surface formed by the soil mass above the tunnel to achieve stability under its own gravity after tunnel excavation, and the included Angle with the horizontal plane is β. After the excavation of the tunnel, a free floor is shaped in the building vicinity of the information tunnel. The soil EFHG above the information tunnel sinks below the motion of gravity, driving the soil EAC and FDB on both sides of the guide tunnel to sink [17]. Due to the cohesion and internal friction Angle provided by inclined plane AC and BD, soil EAC and FDB are restricted to sink, which leads to the subsidence of soil EFHG constrained, and finally, soil ACBD reaches the ultimate equilibrium state. Since the soil strength parameter of the contact surface between EFHG and the triplet on both sides is unknown, the friction Angle θ of the sliding surface is given by experience, and the fee θ influences the accuracy of the calculation consequences of surrounding rock strain [18].

3.2 Calculation and Derivation of Surrounding Rock Pressure

It is assumed that the failure modes of loess tunnels are symmetrically dispensed and the soil electricity parameters inside the failure vary of caves are additionally symmetrically distributed. In structural mechanics, the anti-symmetric internal force of a positive symmetrical structure is 0, so there is no axial shear stress along the axis of symmetry [19]. In order to simplify the calculation, 1/2 of the failure mode of the cavern was taken for force analysis, as shown in Figure 3.

In order to reduce an error caused by θ friction Angle of the sliding surface between EAC and EMNG, the overall force analysis of EAC and EMING is carried out [20]. ACGNME is taken as the soil mass for overall force analysis. The force vector diagram is shown in Figure 3. The excavation route of the information tunnel is 1 *m*, and the pressure stability equation is hooked up in accordawithe to Figure 3, as proven in Equation (3):

$$W_1 + W_2 - Q = (E_0 + e)\cot(\beta - \varphi) \tag{3}$$

Where, W_1 is the gravity of the soil EMNG above the information tunnel, *kN*; W_2 is the gravity of EAC, *kN*; Q is the whole cost of vertical stress appearing on the NG plane, *kN*; E_o is the whole cost of static earth stress on the central axis, *kN*; *e* is the whole fee of lateral earth strain performing on the aiding structure, *kN*; β is the Angle between the sliding airplane AC and the horizontal plane, (°); φ is the interior friction Angle of the soil, (°).

The dead weight of ACGNME is shown in Equation (4) [21]:

$$W_1 + W_2 = \gamma HB + \frac{1}{2}\gamma(H + h)\frac{H + h}{\tan\beta} \tag{4}$$

Where, γ is the soil weight, (*kN/m*^{3}); *H* is the buried depth of the tunnel, *m*; *B* is 1/2 of the width of tunnel excavation, *m*; *h* is the height of tunnel excavation, *m*.

The total value of vertical pressure acting on the NG plane is shown in Equation (5):

$$Q = qB \tag{5}$$

Where: *q* is the vertical surrounding rock stress performing on NG aircraft (*kPa*).

The total lateral earth pressure is shown in Equation (6) [22]:

$$e = \lambda qh \tag{6}$$

Where λ is the coefficient of lateral pressure.

Static earth strain is proven in Equation (7) [23]:

$$E_0 = \int_0^H K_0 \gamma z \, \mathrm{d}z = \frac{1}{2} K_0 \gamma H^2 \tag{7}$$

Where K_o is the pressure coefficient of static earth.

Equation (8) can be obtained by connecting lines (3) to (7):

$$qB = \gamma H B + \frac{1}{2}\gamma (H+h)^2 \cot\beta - \left(\frac{1}{2} K_0 \gamma H^2 + \lambda q h\right) \cot(\beta - \varphi) \tag{8}$$

The analytical formula of the pressure of loose surrounding rock acting on the NG plane is obtained, as shown in Equation (9):

$$q = \gamma H \frac{B + \frac{1}{2}\left(1 + \frac{h}{H}\right)(h+H)\cot\beta - \frac{1}{2} K_0 H \cot(\beta - \varphi)}{B + \lambda h \cot(\beta - \varphi)} \tag{9}$$

If q is regarded as a function of H, Equation (10) can be obtained:

$$\lim_{H \to 0} q(H) \neq 0 \tag{10}$$

That is, when the tunnel buried depth is 0, the surrounding rock stress appearing on the aiding shape is no longer 0, which is inconsistent with the proper state of affairs [24]. Therefore, Equation (9) is modified to gain the analytical equation of vertical unfastened surrounding rock strain appearing on the NG plane, as proven in Equation (11):

$$q = \gamma H \frac{B + \frac{1}{2}(h+H)\cot\beta - \frac{1}{2} K_0 H \cot(\beta - \varphi)}{B + \lambda h \cot(\beta - \varphi)} \tag{11}$$

The analytical formula of horizontal surrounding rock pressure is shown in Equation (12):

$$q_{\mathrm{h}} = \lambda q \tag{12}$$

Where, q_h is the horizontal surrounding rock strain on the helping structure, *kPa*.

From Equation (11), it can be viewed that the vertical surrounding rock stress q is a quadratic characteristic of tunnel burial depth H, $\frac{\partial q}{\partial H} = 0$.

When the vertical surrounding rock pressure is q_{max}, the tunnel burial depth H_{max} can be obtained, as shown in Equation (13):

$$H_{\max} = \frac{B + h\cot\beta}{K_0\cot(\beta-\varphi) - \cot\beta} \tag{13}$$

According to the limit equilibrium theory, after tunnel excavation, soil ACGNME is just in a critical equilibrium state, and there is no vertical earth pressure above the tunnel, and the corresponding tunnel burial depth is denoted as H_o, so Formula (14) can be written as follows:

$$P = 0 \Leftrightarrow W_1 + W_2 - F\cos(\beta-\varphi) \tag{14}$$

According to the triangle sine theorem shown in Figure 3, Equation (15) can be obtained:

$$\frac{F}{\sin 90^\circ} = \frac{E_0 + e}{\sin(\beta-\varphi)} \tag{15}$$

After simplification, it is shown in Equation (16):

$$K_0 H\cot(\beta-\varphi) = 2B + (H+2h)\cot\beta \tag{16}$$

Formula (17) is obtained:

$$H_0 = H = \frac{2(B + h\cot\beta)}{K_0\cot(\beta-\varphi) - \cot\beta} = 2H_{\max} \tag{17}$$

Therefore, when the tunnel burial depth $H \in (0, H_{max})$, the surrounding rock stress performing on the helping form will expand with the tunnel burial depth. When the tunnel burial depth is H_{max}, the surrounding rock pressure performing on the assisting structure reaches the most value, and the soil above the tunnel reaches the closing equilibrium state, that is, the tunnel is in the most unstable state. Since the tunnel burial depth $H \in (H_{max}, H_o)$, the surrounding rock pressure acting on the assisting structure decreases with the amplify of tunnel burial depth, this is due to the truth the mechanical homes of soil step through step get greater with the prolonged of tunnel burial depth [25]. When the tunnel buried depth is Ho, the soil above the tunnel definitely reaches the critical balance, and no surrounding rock pressure acts on the supporting structure. However, the buried depth of tunnel $H \in (H_o, \infty)$, the surrounding rock stress received through the new strategy is negative, which is inconsistent with the perfect situation. Therefore, the surrounding rock stress precept applicable to deep buried tunnel wants to be selected,

so H_{max} is the boundary depth of the deep and shallow buried tunnel. The boundary depth between deep and shallow buried tunnels bought through Equation (17) is ordinarily decided with the aid of tunnel excavation width *B*, peak *h*, soil interior friction Angle φ, and static soil stress coefficient K_o.

3.3 Derivation of Theoretical Calculation Formula of Surrounding Rock Fracture Angle

As can be seen from Equation (11), bodily and mechanical parameters of a precise tunnel are determined, and only a rupture Angle β needs to be determined. According to the theoretical calculation of Terzaghi and Rankine soil pressure, the fracture Angle in the loose body is $\beta = \pi/2+\varphi$. For this calculation formula, Bill Bowman gave the theoretical derivation process [26]. However, the actual fracture Angle of the loess tunnel is obviously greater than the calculated value of this formula. Therefore, the system is derived in the stress country of the sliding floor of the surrounding rock.

In the loess tunnel fracture Angle calculation model, σ_l' and σ_3' are the vertical stress and horizontal stress of the unique rock after conversion, *kPa*; σ_n and τ_n are the normal stress and shear stress on the fracture surface in *kPa*. In practical engineering, when the soil is excavated and a free surface is formed, the gravity of BB'IE soil is transferred to the right soil JJ'B in the form of additional stress by the contact force between soils (cohesion *c*, internal friction Angle φ, etc.). Let's start with the following assumptions:

(a) According to the ratio of an area of the upper soil column EBB'I to the area of the lower triangle soil strip JJ'B, the weight of the upper soil column is equivalent to that of the lower triangle soil strip JJ'B, and the equivalence coefficient is $\frac{2h(b\tan\beta+H)}{H^2}$;
(b) The common collapse surface of loess tunnel is vertical type, so the influence of shadow soil rotation on σ_1 is ignored [27].
(c) The irregular shape of the tunnel section is reduced to a rectangle.

The gravity of BB'IE soil mass is averaged. Based on the above assumptions, the stress subject of JJ'B 'triangle soil mass at the decreased proper aspect beneath the motion of extra stress is equal to:

$$\sigma_3' = \sigma_3\left[1 + \frac{2h(b\tan\beta + H)}{H^2}\right] \tag{18}$$

$$\sigma_1' = \sigma_1 \tag{19}$$

And there is,

$$\sigma_1' = \lambda\sigma_3' \tag{20}$$

In the formula, σ_1 and σ_3 are the vertical stress and horizontal stress of the original rock before the equivalent, *kPa*.

The relationship between the primary rock stress at any point on the sliding fracture surface is:

$$\begin{cases} \sigma_{\mathrm{n}} = \sigma_3' \sin^2\beta + \sigma_1' \cos^2\beta \\ \tau_{\mathrm{n}} = (\sigma_3' - \sigma_1') \sin\beta\cos\beta \end{cases} \tag{21}$$

And the limit of ultimate shear strength on the sliding surface is [28]:

$$\tau_{\max} = \sigma_{\mathrm{n}} \tan\varphi + c \tag{22}$$

Let function $O(\beta)$ be the difference between the ultimate shear strength function and shear stress on the sliding crack surface [29], i.e.:

$$O(\beta) = \tau_{\max} - \tau_{\mathrm{n}} \tag{23}$$

By substituting Equations (20)–(22) into Equations (23), we can get:

$$O(\beta) = (\sigma_3' \sin^2\beta + \sigma_1' \cos^2\beta)\tan\varphi + c - (\sigma_3' - \sigma_1')\sin\beta\cos\beta \tag{24}$$

Tunnels are most dangerous when the first derivative of $O(\beta)$ with respect to beta is zero. Thus, taking the derivative of Equation (24) and considering $K = H/2b$, the formula for calculating the rupture Angle when the tunnel is most dangerous can be written as follows:

$$\tan(2\beta) = \frac{\frac{h}{KH} + (1-\lambda)\tan\varphi}{-\frac{2h}{H} + (\lambda - 1) + \frac{h}{KH}\tan\varphi} \tag{25}$$

4 Reasonableness Verification and Parameter Influence Analysis of Surrounding Rock Pressure

4.1 Verification of Rupture Angle Rationality

Six loess tunnels in Hejiazhuang and Lujiayan of Zhengxi Tourist Site are selected, and their bodily and mechanical parameters and burial depth are proven in Figure 4. The excavation height and span of the six tunnels were the same, $H = 13.38m$, $D = 15.4m(D = 2b)$. The lateral pressure coefficient λ is calculated according to the "Code for Design of Railway

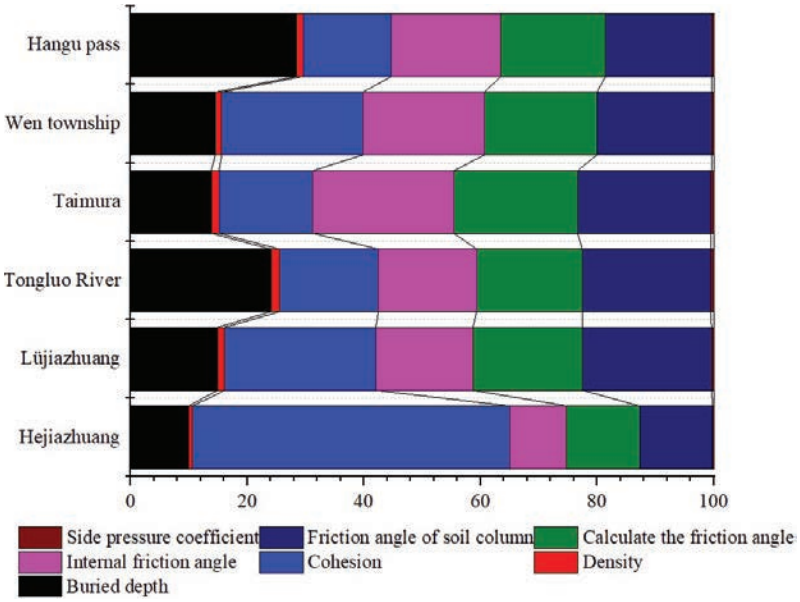

Figure 4 Parameters of each tunnel.

Tunnel", and the results are also shown in Figure 4. The common value θ of the friction angle of the soil column was selected according to the Code for Design of Railway Tunnel [30], $\theta = 0.9\phi_c$ for grade IV surrounding rock and $\theta = 0.7\phi_c$ for grade V surrounding rock. The results are also shown in Figure 4. Respectively using the method, Xie Jiayi method, sand,and Bill Bowman, about six tunnel burst Angles are calculated separately, and the beta, results are shown in Figure 5. At the same time, the actual rupture Angle β of the six tunnels was measured, and the distinction between the theoretical fee and the measured fee was once calculated. The consequences are proven in Figure 5.

From Figure 5, it can be seen that the difference between the fracture angle calculated by the Xie Jiayi method and the measured value is $-6.5°\sim1.6°$, and the difference between the method in this paper and the measured value is $-2.3°\sim1.2°$. It can be seen that the Xie Jiayi method and the method in this paper are close to the measured value in the field, and the difference between the method in this paper is smaller; At the same time, the friction angle of the soil column in Xie Jiayi method θ the value has a great influence on the result, and it is taken under the condition of Class IV surrounding rock $\theta = 0.7\varphi_c\sim0.9\varphi_c$. Taken under the condition

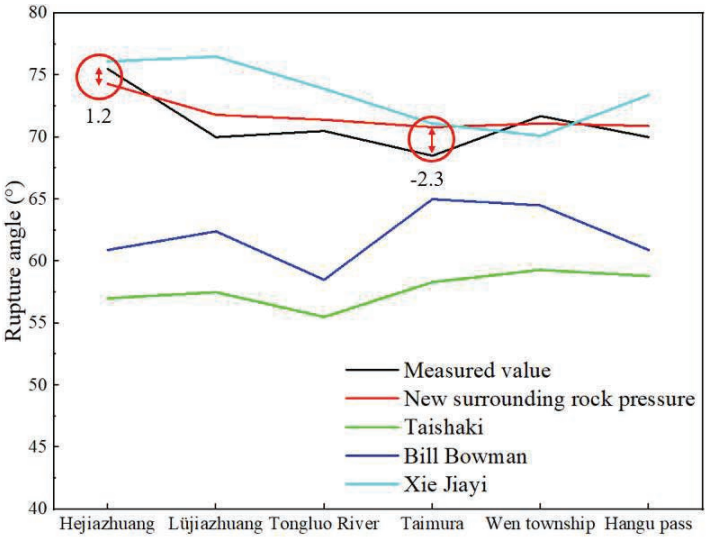

Figure 5 Burst Angle calculation results of the validation.

of Class V surrounding rock $\theta = 0.5\varphi_c \sim 0.7\varphi_c$. The difference between the calculated fracture angles is 7.7° and 3.1° respectively, and this value method is completely based on experience and has not been verified by theory. Therefore, the results of the Xie Jiayi method are subject to human subjective factors [31]. The difference in fracture angle obtained by the Bill Bowman method is 3.5°∼14.6°, and Taishaki is 10.3°∼18.5°, both are far greater than the difference of the method in this paper.

Taking Hejiazhuang Tunnel as an example, when a single parameter changes, its values are as follows: lateral pressure coefficient $\lambda = 0.4, 0.5 \ldots, 1.5$; Internal friction Angle $\varphi = 5°, 10° \ldots 45°$, Cross section vector span ratio (flat-rate) $K = 0.5, 0.6 \ldots, 1.5$; Tunnel buried depth $h = 10, 15, \ldots, 50\ m$. Respectively using the method, Taishaki, Bill Bowman, and Xie Jiayi method, analysis of the four single parameter changes on the influence of the rupture Angle beta, as shown in Figures 6–9.

The following conclusions can be drawn from Figures 6–9.

(a) The rupture perspective calculated via the technique of this paper and the Xie Jiayi technique decreases slowly with the make bigger the lateral strain coefficient, i.e., the impact is now not very obvious. The calculated rupture attitude of the Taisaki technique is impartial to the lateral stress coefficient. The calculated rupture perspective of the Bill Bowman approach will increase with the make bigger aspect stress coefficient

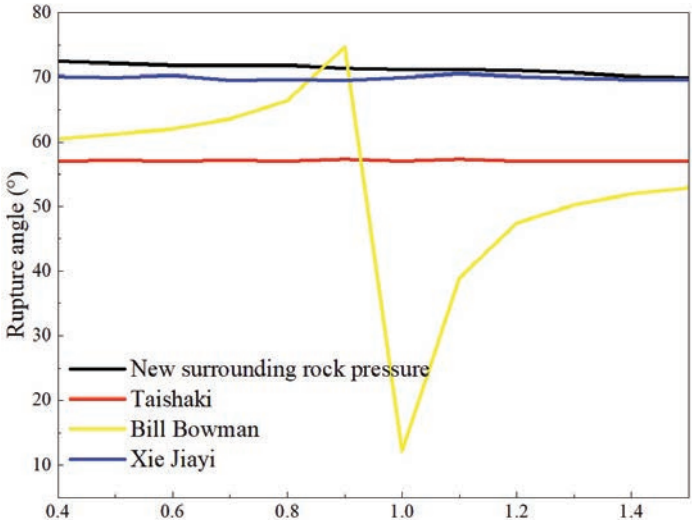

Figure 6 Pressure coefficients on different sides.

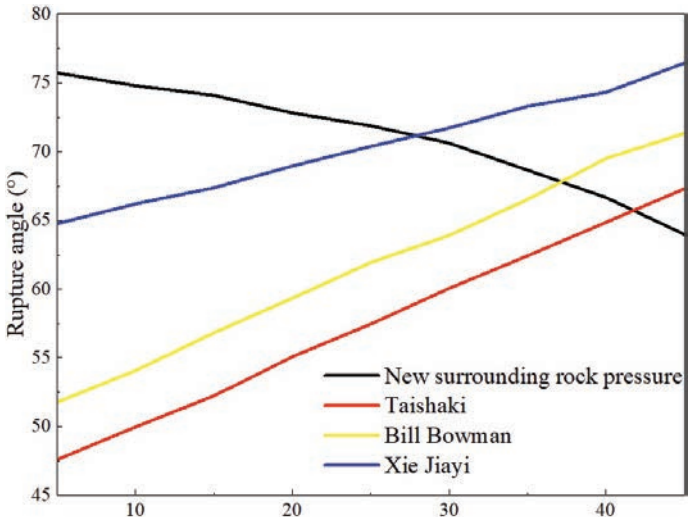

Figure 7 Different internal friction angles.

when the aspect strain coefficient is much less than 0.9, and the price of expexpansionll increase continuously, whilst the rupture perspectill of suddthe en decreases when the facet stress coefficient is 1.0; the calculated rupture attitude will increase with the expand of aspect stress

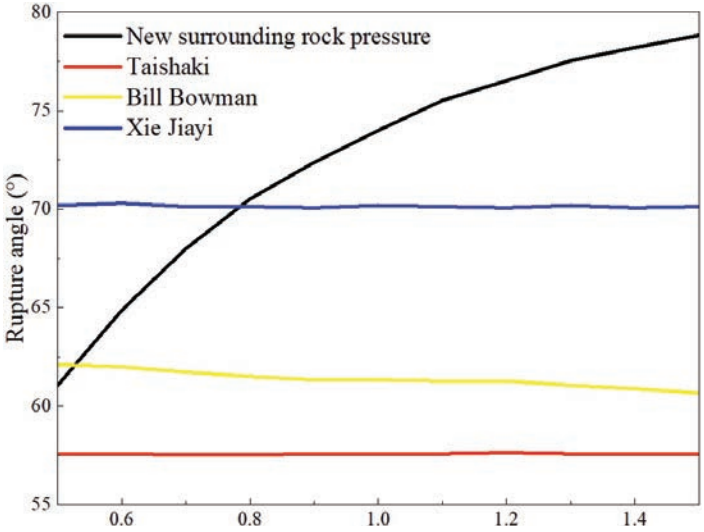

Figure 8 Different vector span ratios.

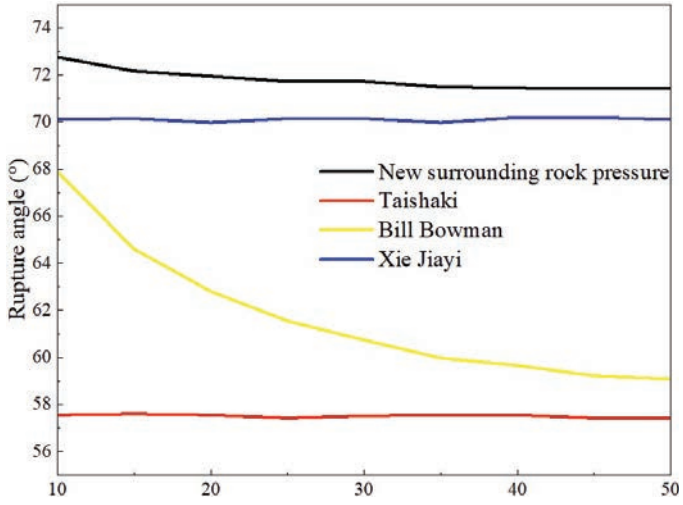

Figure 9 Different tunnel depths.

coefficient when the facet stress coefficient is larger than 10, and the charge of extend decreases continuously.

(b) The rupture perspective calculated by using the technique in this paper decreases with the make bigger inside friction angle, whilst the rupture attitude calculated by way of the Taisaki method, Bill Bowman

approach, and Xie Jiayi approach will increase with the expansion of interior friction angle. The genuine rupture perspective of the discipline lookup tends to reduce with the amplification of the interior friction angle.

(c) The rupture perspective calculated via this approach will increase with the amplification of vector-to-span ratio, whilst the rupture perspective calculated by way of the different three techniques no longer trade much.

(d) The rupture perspective calculated via this technique decreases slowly with the enlarging of tunnel burial depth till it is stable, the rupture perspective calculated by way of the Taisaki technique and Xie Jiayi technique is no longer associated with the tunnel burial depth, and the rupture attitude calculated by using Bill Bowman technique decreases extensively with the expand of tunnel burial depth.

(e) In a comprehensive view, the rupture angle of the calculation method in this paper is most obviously influenced by the vector-to-span ratio and the internal friction angle, which is most consistent with the actual situation of the shallowly buried loess tunnel and verifies the reasonableness and correctness of the method in this paper.

4.2 Verification of the Reasonableness of the Surrounding Rock Pressure

Referring to the survey and diagram information of the Hejiazhuang tunnel, the soil potential of the loess tunnel is taken as 18 kN/m^3, the inside friction attitude is taken as 25°, the cohesive pressure is taken as 30 kPa, the tunnel span is taken as 14.72 m, the tunnel peak is taken as 12.58 m, and the static earth strain coefficient K_o is taken as 0.58 (calculated in accordance to the empirical formulation in the Technical Specification for Building Foundation Engineering). Set the tunnel burial depth of 0∼120 m, the calculated new mannequin of the surrounding rock stress and the relationship between the tunnel burial depth is proven in Table 2. As can be considered from Table 2, the new mannequin of the surrounding rock strain effects between the Bill Bowman formulation and Taisaki formula, and with the expansion in depth of burial is a parabolic structure of change. The height stress of the surrounding rock seems in the burial depth between 60∼70 m, after exceeding the height burial depth, the surrounding rock stress decays rapidly, and when the tunnel burial depth exceeds a positive range, the surrounding rock strain will even show up negative, which is now not steady with the real engineering. Therefore, this technique is appropriate for shallow buried tunnel rock stress

Table 2 The new mannequin calculates the relationship between the surrounding rock strain and the deep burial of the tunnel

Buried Deep	New Surrounding Rock Pressure	Taishaki	Bill Bowman	Xie Jiayi	Specification
0	0	0	0	0	0
5	71.538	56.862	85.614	77.976	78.676
10	141.323	120.205	151.877	165.953	165.953
15	211.701	180.029	218.739	246.891	246.891
20	260.968	225.777	275.044	317.273	296.158
25	324.311	264.487	352.463	387.654	370.059
30	367.84	303.196	401.73	465.073	422.845
35	412.287	331.349	450.997	528.416	479.15
40	443.959	359.501	510.821	588.24	528.416
45	475.63	380.616	542.493	644.545	570.645
50	503.783	406.149	570.645	693.812	609.355
55	524.897	415.806	598.798	746.598	641.026
60	535.455	429.883	626.95	799.384	669.179
65	538.974	443.959	644.545	838.094	693.812
70	535.455	458.035	648.065	869.765	707.889
75	535.455	461.554	655.103	904.956	718.446
80	528.416	475.63	662.141	933.109	718.446
85	507.302	472.111	651.584	971.818	725.484
90	486.188	493.226	644.545	982.375	711.408
95	458.035	486.188	623.431	1014.05	697.331
100	426.764	493.226	595.279	1028.12	677.817

calculation, the top strain of the surrounding rock corresponding to the burial depth is deep shallow burial necessary burial depth.

The bodily and mechanical parameters of the three tunnels are proven in Figure 4, and the excavation peak and span are nevertheless $H = 13.38\,m$ and $D = 15.4\,m$ $(D = 26)$. Because the vicinity of the website survey to reveal the surrounding rock strain and the place of the survey rupture perspective is now not equal place, the burial depth of the tunnel is proven in Table 3. the technique of this paper and the aspect stress coefficient of the Taishaki technique are chosen in accordance to the measured values on site, and the aspect strain coefficient of the Xie Jiayi approach is calculated in accordance to the applicable components of the Railway Tunnel Design Code, and the effects are proven in Table 3. the friction attitude θ of the soil column of the Xie Jiayi technique is chosen in accordance to the code, the classification IV surrounding rock $\theta = 0.8\phi_c$, V surrounding rock $\theta = 0.6\phi_c$. The measured and calculated values of the surrounding rock strain are proven in Table 3.

Table 3 Comparison of the calculated results of the pressure in the loess tunnel envelope

	Measured Value		New Surrounding Rock Pressure		Bill Taishaki		Bill Bowman		Xie Jiayi	
Tunnel	V	H	V	H	V	H	V	H	V	H
Hejiazhuang	186.7	276.5	210.7	301.4	177.8	124.1	427.2	234.8	305.7	261.1
Tongluo River	247.6	311.6	298.4	385.9	349.3	235.9	487.5	269.7	416.7	216.5
Hangu pass	126.3	163.4	145.6	198.4	230.5	124.2	354.1	168.2	324.5	146.8

From Table 3, we can see that: for vertical rock pressure, the calculated value of the Taishaki method for the Hejiazhuang tunnel is smaller than the measured value in the field, because the Taishaki method does not consider the effect of a cohesive force, and it is unsafe to design support based on it, so Taishaki technique can't be used to calculate the strain of shallowly buried loess tunnel; the calculated values of Xie Jiayi method, Bill Bowman method, Taishaki technique for the different two tunnels and this technique are large than the measured cost in the field, however, the calculated cost of this technique is nearer to the measured value. However, the calculated cost of this technique is nearer to the measured value; for the horizontal rock pressure, the two tunnels of Xie Jiayi, Taishaki, and Bill Bowman approach are smaller than the measured cost in the field, so it is risky to layout assist based totally on this method; the vertical and horizontal rock stress calculated by using this technique is large than the measured price in the field, which has a sure protection reserve, and the vertical rock strain is drastically smaller than that of Xie Jiayi and Bill Bowman method. Therefore, the technique in this paper is right and fine for calculating the surrounding rock stress of sa hallow buried loess tunnels.

4.3 Analysis of the Influence of Parameters on the Calculated Value of the Surrounding Rock Pressure

Only the variation of vertical rock pressure with a single parameter is analyzed here. Taking the Hejiazhuang tunnel as an example, the values of single parameters are taken as follows: lateral pressure coefficient $\lambda = 0.8, 1.0, \ldots, 2.0$; internal friction angle $\varphi = 15°, 20°, \ldots, 45°$; section vector-to-span ratio (flatness) $K = 0.6, 0.8, \ldots, 2.0$, where the tunnel excavation span $D = 15.4\ m$ constant, the height takes different values; tunnel burial depth $h = 15, 20, \ldots, 45\ m$; cohesion $c = 0, 10, \ldots, 100$ *kPa*; gravity $\gamma = 15, 17, \ldots, 21$ *kN/m*^{3}; calculated friction angle $\varphi_c = \varphi + 10°$, and Soil column friction angle $\theta = 0.7\varphi_c$. The effect regulation of these six single

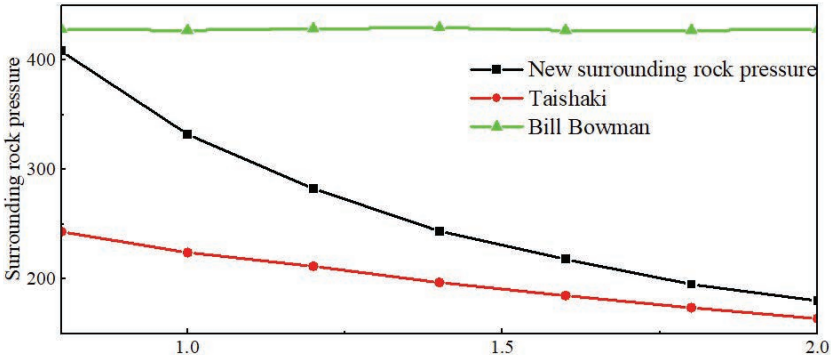

Figure 10 Different pressure measurement coefficients.

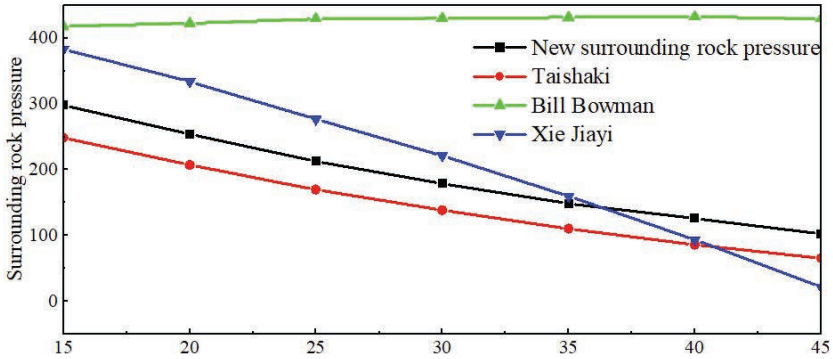

Figure 11 Different internal friction angles.

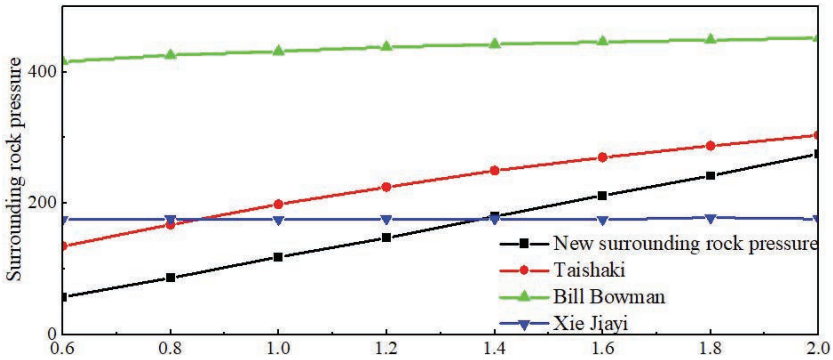

Figure 12 Different vector span ratios.

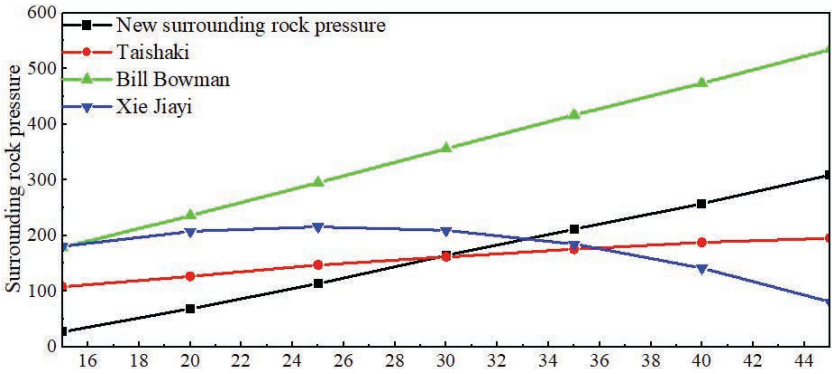

Figure 13 Different tunnel depths.

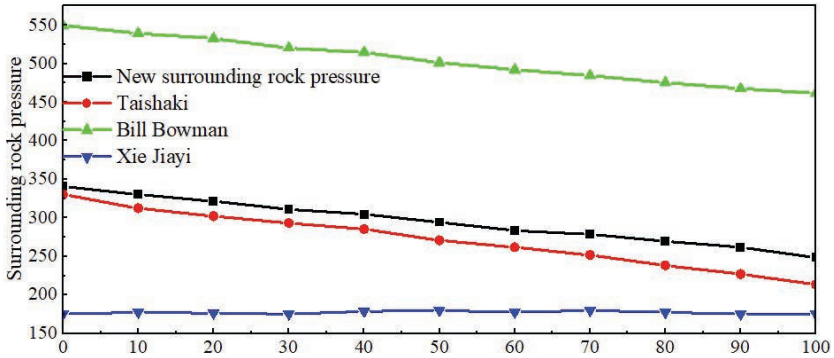

Figure 14 Different cohesion.

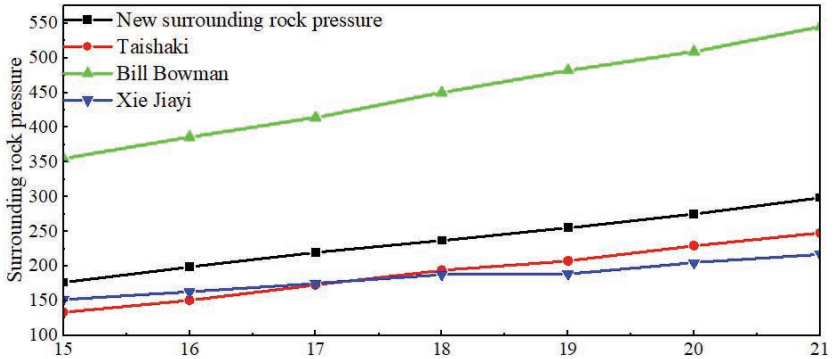

Figure 15 Different severity.

parameter adjustments on the vertical surrounding rock strain is analyzed by using the technique of this paper, Xie Jiayi method, Taishaki approach, and Bill Bowman approach respectively, as proven in Figures 10–15. The following conclusions can be acquired from the figure.

(a) The lateral strain coefficient acquired through the Xie Jiayi technique is typically much less than 1.0, whilst the current lateral strain coefficients of loess tunnels are normally dispensed between 0.8 and 2.0, so the Xie Jiayi technique is no longer analyzed. With the make bigger lateral strain coefficient, the circumferential strain calculated by using the approach of this paper and Taishaki approach progressively decreases, whilst that of Bill Bowman's approach is nearly unchanged.

(b) With the make bigger the inside friction angle, the stress of the surrounding rock calculated with the aid of this approach and Xie Jiayi approach are non-linearly decreasing, while the Taishaki method is linearly decreasing, and the Bill Bowman method is slowly increasing and then slowly decreasing.

(c) With the increase of vector-span ratio, the surrounding rock pressure calculated by this method, Taishaki method, and Bill Bowman method gradually increases, while that of Xie Jiayi method does not change, obviously Xie Jiayi method ignores the role of vector-span ratio on surrounding rock pressure, which means that Xie Jiayi method is not comprehensive.

(d) With the enlargement of tunnel burial depth, the surrounding rock strain calculated via the technique of this paper, the Taishaki approach and the Bill Bowman technique will increase linearly, and the Xie Jiayi approach will increase first and then decreases.

(e) With the increase of cohesion, the surrounding rock pressure calculated by this paper, Taishaki method, and Beer Baumann method decreases linearly, but there is no change in the Xie Jiayi method, which means that the calculation result of the Xie Jiayi method does not conform to the actual law.

(f) With the increase of heaviness, the surrounding rock pressure calculated by the four methods is linearly increased and the increase is basically the same.

(g) In summary, it can be considered that the calculated values of the surrounding rock stress of the strategies in this paper differ. The alternate of parameters is in accordance with the well-known rule, the Xie Jiayi technique can't completely think about the have an effect on cohesion,

vector-to-span ratio and lateral stress coefficient, the circumferential stress calculated with the aid of the Taishaki technique is much less than the measured fee in the field, and the circumferential strain calculated with the aid of the Bill Bowman technique is too giant and can't replicate the have an effect on of the lateral strain coefficient on the circumferential pressure, it can be viewed that the technique in this paper can excellently meet the true state of affairs of shallowly buried loess tunnel project, the calculated price of circumferential stress and the calculated values and the actual. The calculated values and the measured values match properly and have a sure security reserve.

5 Conclusion

In this paper, based on the limit equilibrium theory, a circumferential pressure calculation formula applicable to shallow buried loess tunnels is deduced. It is also compared with four theories, namely, Taishaki theory, railroad tunnel design code, Bill Bowman method, and Xie Jiayi method, to verify the reasonableness and superiority of the newly proposed method for calculating the surrounding rock pressure in loess tunnels in this paper. The influence law of various parameters on the surrounding rock pressure and rupture angle is also further considered. The specific results are as follows.

(1) To summarize the damage pattern of the loess tunnel, the damage characteristics are as follows: the rupture surface of the loess tunnel is composed of two parts, namely, the lower inclined closed shear crack and the upper vertical tension crack, both of which form an "inverted eight" type in the distribution of the soil body; the location of the surface crack moves away from the tunnel axis and to both sides with the increase of the tunnel burial depth, and the surface The inclination of the shear slip surface at the lower part of the tension cracks is slightly more than $45^\circ + \varphi/2$.
(2) In this paper, based on the existing theory of perimeter rock pressure, the influence of lateral earth pressure, static earth pressure, tunnel size, tunnel depth, and soil parameters on the perimeter rock pressure is considered.
(3) Comparing the new method, the existing theory, and the field monitoring values, the field monitoring values are smaller than the vertical and lateral rock pressure calculated by the new method and the existing theory, but the error of the new method is relatively small and can be

used for the calculation of the rock pressure in shallow buried cut-and-cover tunnels in loess strata. The proposed method is negatively related to the lateral pressure coefficient, internal friction angle, and cohesion, and positively related to the vector-to-span ratio, tunnel depth, and soil weight, but with the increasing depth of the tunnel, there is a peak of the surrounding rock pressure, and the surrounding rock pressure curve is increasing and then decreasing.

The monitoring sections arranged in this paper are limited, and the measurement points arranged in each section are limited, resulting in the sample of monitoring data is not large enough, and the monitoring results may appear certain chance. Subsequently, we can consider enriching the monitoring content and increasing the number of monitoring sections and points, so as to obtain a larger sample of monitoring data and conduct a more in-depth study on the forces of the surrounding rock and the supporting structure.

References

[1] Sun W, Liang Q, Qin S, et al. Evaluation of groundwater effects on tunnel engineering in loess[J]. Bulletin of Engineering Geology and the Environment, 2021, 80: 1947–1962.

[2] Zhao Y, He H, Li P. Key techniques for the construction of high-speed railway large-section loess tunnels[J]. Engineering, 2018, 4(2): 254–259.

[3] Xiao X, Yangbing Z, Xin W. Prediction Method of Characteristic Value of Foundation Bearing Capacity Based on Machine Learning Algorithm[J]. European Journal of Computational Mechanics, 2022: 197–216.

[4] Jin Zhengfu, Fu Daxi, Yang Minghui, et al. Loose pressure limit analysis of shallow buried tunnels considering the structural properties of loess [J]. Highway and Transportation Technology, 124–131.

[5] Wang H, Jiang H, Yang F. Study on the Mechanical Properties of Hydraulic Tunnels With High Ground Temperature and the Temporal and Spatial Evolution of Plastic Zone[J]. European Journal of Computational Mechanics, 2021: 145–168.

[6] Shao, S.J., Deng, G.H. Structural strength properties of in-situ loess and its application to the pressure analysis of loess tunnel envelope[J]. Journal of Civil Engineering, 2008, 41(11): 93–98.

[7] Bagheri H, Kiani Y, Eslami M R. Asymmetric compressive stability of rotating annular plates[J]. European Journal of Computational Mechanics, 2019: 1–21.
[8] Hu Zhenbao. Calculation method of loose surrounding rock pressure in shallow buried tunnel in loess area and its application[D]. Hunan University, 2021.
[9] Wang L, Li C, Qiu J, et al. Treatment and effect of loess metro tunnel under surrounding pressure and water immersion environment[J]. Geofluids, 2020, 2020: 1–18.
[10] Shao S, Shao S, Li J, et al. An Analysis of Loess Tunnel Failure and Its Mechanism[J]. Advances in Civil Engineering, 2021, 2021: 1–18.
[11] Qiu J, Lu Y, Lai J, et al. Experimental study on the effect of water gushing on loess metro tunnel[J]. Environmental Earth Sciences, 2020, 79: 1–19.
[12] Hu Z, Zhang J, Yang Y, et al. Study on the Surrounding Rock Pressure Characteristics of Loess Tunnel Based on Statistical Analysis in China[J]. Applied Sciences, 2022, 12(13): 6329.
[13] Li J, Shao S, Shao S. Collapsible characteristics of loess tunnel site and their effects on tunnel structure[J]. Tunnelling and Underground Space Technology, 2019, 83: 509–519.
[14] Wu Feijie, Shao Shengjun, She Fangtao. Research on a limit equilibrium theory calculation method for the pressure of loess tunnel envelope[J]. Journal of Xi'an University of Technology, 2016, 32(3): 338–342.
[15] Zhao M, Lai H, Liu Y. A Study on the Formation Mechanism and Calculation Method of Surrounding Rock Pressure in Shallow-buried Loess Tunnel Considering the Influence of Vertical Joints[J]. KSCE Journal of Civil Engineering, 2023: 1–18.
[16] Qiu J, Lu Y, Lai J, et al. Failure behavior investigation of loess metro tunnel under local-high-pressure water environment[J]. Engineering Failure Analysis, 2020, 115: 104631.
[17] Wang Chunhao. Analysis of pressure calculation method for the surrounding rock of super large section loess highway tunnel[J]. Modern Tunnel Technology, 2015, 52(3): 175–181.
[18] Fan H, Liu T, Zhang S, et al. Effects of Jet-Grouting Piles on Loess Tunnel Foundation with Centrifugal Model Tests[J]. International Journal of Geomechanics, 2023, 23(3): 04022298.
[19] Wang D, Luo J, Shen K, et al. Analysis of the causes of the collapse of a deep-buried large cross-section of loess tunnel and evaluation of treatment measures[J]. Applied Sciences, 2022, 12(1): 161.

[20] Dai J, Yang K, Shang Xexuan, et al. Calculation of loose surrounding rock pressure in shallow buried concealed tunnels with loess strata[J]. China Safety Production Science and Technology, 2022.
[21] Luo Y, Chen J, Shi Z, et al. Mechanical characteristics of primary support of large span loess highway tunnel: a case study in Shaanxi Province, Loess Plateau, NW China primary[J]. Tunnelling and Underground Space Technology, 2020, 104: 103532.
[22] Shi W, Qiu J, Zhang C, et al. Immersion mode and spatiotemporal distribution characteristic of water migration in loess tunnel[J]. Arabian Journal of Geosciences, 2022, 15(7): 654.
[23] Weng X, Sun Y, Zhang Y, et al. Physical modeling of wetting-induced collapse of shield tunneling in loess strata[J]. Tunnelling and Underground Space Technology, 2019, 90: 208–219.
[24] Wang M.N., Guo J., Luo L.S., et al. Calculation method of pressure on the surrounding rock of a large-section deeply buried loess tunnel for high-speed railroad[J]. China Railway Science, 2009, 30(5): 53–58.
[25] Qiu J, Qin Y, Lai J, et al. Structural response of the metro tunnel under local dynamic water environment in loess strata[J]. Geofluids, 2019, 2019.
[26] Xiao Q, Lei S, Cui K, et al. Effect of the longitudinal local wetting-induced collapse on tunnel structure in loess strata[J]. Tunnelling and Underground Space Technology, 2022, 122: 104361.
[27] Yu L, Lv C, Duan Ruyu, et al. Method for calculating pressure in shallowly buried loess tunnel enclosures[J]. China Railway Science, 2019, 40(4): 69–76.
[28] Hu Z, Du K, Lai J, et al. Statistical analysis of influence of cover depth on loess tunnel deformation in NW China[J]. Advances in civil engineering, 2019, 2019.
[29] Li Y, Xu S, Liu H, et al. Displacement and stress characteristics of tunnel foundation in collapsible loess ground reinforced by jet grouting columns[J]. Advances in Civil Engineering, 2018, 2018.
[30] Jian-xun C, Jiu-chun J, Meng-shu W. Function of rock bolt of lattice girder and shotcrete support structure in loess tunnel[J]. China Journal of Highway and Transport, 2007, 20(3): 71.
[31] Weng X, Zhou R, Rao W, et al. Research on subway shield tunnel induced by local water immersion of collapsible loess[J]. Natural hazards, 2021, 108: 1197–1219.

Biographies

Cheng Danjiang received the bachelor's degree in engineering from Shanxi University of Technology in 2005. He is currently working as an senior engineer at China Communication North Road & Bridge Co., Ltd. He research areas and directions include Highway bridge construction, tunnel construction and project management.

Hua Junfeng received the bachelor's degree in engineering from LanZhou Jiaotong University of Technology in 2009. He is currently working as an senior engineer at China Communication North Road & Bridge Co., Ltd. He research areas and directions include Highway bridge construction, tunnel construction and project management.

Zhu Jianguo received the bachelor's degree in engineering from Shandong Jianzhu University of Technology in 2015. He is currently working as an engineer at China Communication North Road & Bridge Co., Ltd. He research areas and directions include Highway bridge construction, tunnel construction and project management.

Ji Yang received the bachelor's degree in engineering from Southeast University in 2015. He is currently working as an head engineer at Jiangsu filiale of The Second Construction Co., Ltd. Of China Construction First Group. He research areas and directions include green construction and engineering project management.

Hu Zhaoguang received the bachelor's degree in engineering from Northeast Forestry University in 2005, the master's degree in engineering from Northeast Forestry University in 2012, and the doctorate degree in engineering from Northeast Forestry University in 2017. He is currently working as an Lecturer at the School of Civil Engineering and Architecture, Zhengzhou University of Aeronautics. His research areas and directions include Highway bridge construction, tunnel construction and project management.